Available online at www.sciencedirect.com
ScienceDirect
Journal of Theoretical Biology 250 (2008) 498–511
Journal of Theoretical Biology
www.elsevier.com/locate/yjtbi

The influence of trade-off shape on evolutionary behaviour in classical ecological scenarios

Andrew Hoyle[a,*], Roger G. Bowers[b], Andrew White[c], Michael Boots[d]

[a]Department of Computing Science and Mathematics, University of Stirling, Stirling, Scotland FK9 4LA, UK
[b]Department of Mathematical Sciences, Division of Applied Mathematics, Mathematical Sciences Building, The University of Liverpool, Liverpool L69 7ZL, UK
[c]Department of Mathematics and the Maxwell Institute for Mathematical Sciences, Heriot Watt University, Edinburgh EH14 4AS, UK
[d]Department of Animal and Plant Sciences, The University of Sheffield, Western Bank, Sheffield S10 2TN, UK

Received 8 June 2007; received in revised form 10 October 2007; accepted 10 October 2007
Available online 12 October 2007

Abstract

Trade-off shapes are crucial to evolutionary outcomes. However, due to different ecological feedbacks their implications may depend not only on the trade-off being considered but also the ecological scenario. Here, we apply a novel geometric technique, trade-off and invasion plots (TIPs), to examine in detail how the shape of trade-off relationships affect evolutionary outcomes under a range of classic ecological scenarios including Lotka–Volterra type and host–parasite interactions. We choose models of increasing complexity in order to gain an insight into the features of ecological systems that determine the evolutionary outcomes. In particular we focus on when evolutionary attractors, repellors and branching points occur and how this depends on whether the costs are accelerating (benefits become 'increasingly' costly), decelerating (benefits become 'decreasingly' costly) or constant. In all cases strongly accelerating costs lead to attractors while strongly decelerating ones lead to repellors, but with weaker relationships, this no longer holds. For some systems weakly accelerating costs may lead to repellors and decelerating costs may lead to attractors. In many scenarios it is weakly decelerating costs that lead to branching points, but weakly accelerating and linear costs may also lead to disruptive selection in particular ecological scenarios. Using our models we suggest a classification of ecological interactions, based on three distinct criteria, that can produce one of four fundamental TIPs which allow for different evolutionary behaviour. This provides a baseline theory which may inform the prediction of evolutionary outcomes in similar yet unexplored ecological scenarios. In addition we discuss the implications of our results to a number of specific life-history trade-offs in the classic ecological scenarios represented by our models.

Keywords: Trade-offs; Shapes; Evolution; Frequency dependence; TIPs

1. Introduction

Life-history theory has long recognised the importance of trade-offs in determining evolutionary behaviour (see Stearns, 1992; Roff, 2002 for reviews). It is also increasingly recognised that the shape of trade-offs, in addition to the level of costs, is crucial in determining the evolutionary dynamics (see Levins, 1962, 1968; de Mazancourt and Dieckmann, 2004; Rueffler et al., 2004; Bowers et al., 2005). By definition, in all trade-off relationships, benefits in one life-history trait come at a cost in terms of another component of fitness. In general then as benefits through one trait increase, the costs due to the change in the other trait may increase at the same rate, leading to an exactly linear trade-off; alternatively the costs may accelerate (increase quicker than the benefits) or decelerate (increase slower than the benefits), so that benefits become increasingly or decreasingly costly. When the benefits of a trait are met with accelerating costs in the correlated trait we define an 'acceleratingly costly trade-off'. Conversely we define 'deceleratingly costly trade-offs' when the costs decelerate. Here our aim is to understand how these different shapes of trade-offs influence evolutionary outcomes in a range of

*Corresponding author. Tel.: +44 1786 467 467; fax: +44 1786 464 551.
E-mail addresses: A.Hoyle@maths.stir.ac.uk (A. Hoyle), sx04@liv.ac.uk (R.G. Bowers), A.R.White@hw.ac.uk (A. White), M.Boots@sheffield.ac.uk (M. Boots).

0022-5193/$ - see front matter © 2007 Elsevier Ltd. All rights reserved.
doi:10.1016/j.jtbi.2007.10.009

scenarios described by a number of classic ecological models.

The importance of the shape of trade-off relationships was first made clear in the work of Levins (1962, 1968). He developed a graphical technique that plots the fitness landscape from the fitness contours for two traits onto which the trade-off relationship between them is superimposed. Applying these techniques to the evolution of reproductive effort it was shown that the optimal strategy for a trade-off with decelerating costs is at the maximum reproductive effort whereas for a trade-off with accelerating costs it is at an intermediate state (see Stearns, 1992). However, optimisation approaches, such as Levin's are not appropriate, when there is frequency-dependent (density-dependent) selection (Maynard Smith, 1982; de Mazancourt and Dieckmann, 2004; Rueffler et al., 2004; Bowers et al., 2005). Different ecological interactions result in particular feedbacks that may clearly lead to different selection pressures on traits (Abrams, 2001) that in turn depend on the nature of the trade-off connections between traits. Here we will examine how trade-off shapes influence evolutionary behaviour in a number of fundamental ecological models using a geometric approach that incorporates frequency-dependent selection.

Under frequency-dependent selection, the evolution of traits is dependent on the ecological feedbacks in the system since for a mutation to be successful it must be able to invade a population whose ecological characteristics are being determined by the resident strain (Metz et al., 1996; Geritz et al., 1998). Successful mutant invasion necessarily changes the resident and therefore also reshapes the characteristics of the population. This approach has been applied to a number of specific ecological scenarios in which trade-off relationships have been explicitly considered (Boots and Haraguchi, 1999; Kisdi, 2001; Day et al., 2002; Bowers et al., 2003; Egas et al., 2004; de Mazancourt and Dieckmann, 2004; White and Bowers, 2005; Rueffler et al., 2006). In particular, the importance of the trade-off shape in characterising evolutionary behaviour has recently been examined in detail with the development of general geometric methods for analysing the evolutionary dynamics (de Mazancourt and Dieckmann, 2004; Rueffler et al., 2004; Bowers et al., 2005). Rueffler et al. (2004) extended the Levins fitness landscape approach to allow for frequency-dependent selection for specific trade-off functions. This was further extended to enable visualisation of the effect of general trade-off functions on evolutionary outcomes (de Mazancourt and Dieckmann, 2004). The method of trade-off and invasion plots (TIPs) developed by Bowers et al. (2005) and first used in Boots and Bowers (2004) is similar to that of de Mazancourt and Dieckmann (2004) in that it is a geometric technique that allows the visualisation of the role of the trade-off shape. From TIPs given a specific ecological model, it is easy to determine which trade-off shapes (or cost structures) produce for example, evolutionary branching. Although globally the curvature of the trade-off can change sign, for example in sigmoidal trade-offs, TIPs focus on the shape of the trade-off locally about the evolutionary singularity; in this local region the curvature of the trade-off stays relatively constant and hence falls into one of three shapes: decelerating, accelerating or straight (linear).

In this study, we use TIPs to explore which ecological characteristics lead to different evolutionary behaviours with trade-offs of different shapes. We use classic models of increasing ecological complexity in order to reveal the ecological features that underlie four fundamental types of TIPs. By classic we mean Lotka–Volterra-type continuous time models, i.e. where the dynamics are linear in terms of the 'evolving' parameters (those involved in the trade-off) and of order one or two (linear, bilinear or quadratic) in terms of densities. We choose this framework as it underpins many model structures in theoretical ecology. In particular, we examine classical single species models, Lotka–Volterra models that include species interactions with one class of individuals for both species and host–parasite systems with multi-class interactions. These TIPs in turn define all the evolutionary implications of different trade-off shapes. In this way we outline how the incorporation of additional ecological mechanisms can alter the topology of the invasion boundaries on a TIP and therefore also the possible evolutionary outcomes. For our range of models, we classify, by means of three criteria, the necessary general ecological characteristics and trade-off set-up required to produce different types of evolutionary behaviour. By focussing on the classical models that underpin much ecological theory, our aim is to provide a baseline that may inform the understanding of more complex ecological scenarios that can be modelled by these type of systems.

2. The approach: trade-off and invasion plots

A detailed description of the use of TIPs to determine evolutionary behaviour has been given elsewhere (Bowers et al., 2005) and their derivation is outlined in Appendix A. An example of a TIP showing its key features can be seen in Fig. 1 (where Table 5 (see Appendix A) has been used to determine whether a region is ES or CS). The mutant–resident invasion boundaries (f_1, f_2) are plotted in trait space and the trade-off line (f) is superimposed such that the position of the trade-off line in relation to the invasion curves determines the evolutionary behaviour. The main advantage of the approach is the relatively easy way in which the nature of the evolutionary outcome can be determined. Thus in Fig. 1, we can immediately see that the evolutionary singularity (the point at the top right hand corner of the TIP in this case, where the fitness gradient is zero) is a branching point (the trait will be selected to move towards the point and then branch because the trade-off curve f enters the TIP in the region where x^* is convergent stable (CS) but not resistant to invasion and therefore not evolutionarily stable (ES)). The evolutionary behaviour of other trade-off curves can also be determined from the TIP.

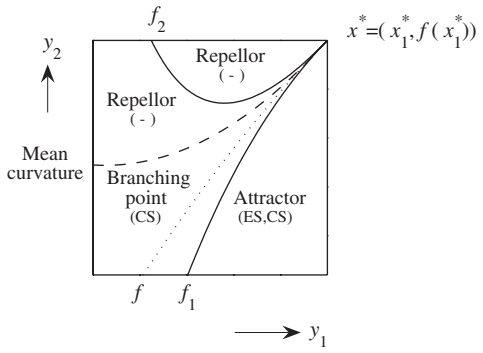

Fig. 1. Example of a singular TIP, displaying the coincidence and mutual tangential property of the trade-off f and two invasion boundaries f_1 and f_2 (denoting where $s_x(y)=0$ and $s_y(x)=0$, respectively) at the tip of the singular TIP (i.e. the top right corner where here $y=x=x^*$). The evolutionary behaviour in each region, deduced from the evolutionary properties is also shown. The actual evolutionary behaviour exhibited by the evolutionary singularity x^* is determined by which region the trade-off curve enters, for example, here the evolutionary singularity is a branching point (the singular point is convergence stable (CS) but not evolutionary stable (ES)). The evolutionary outcome of different trade-off shapes can also be considered. If the curvature of the trade-off was such that it entered the TIP below the f_1 line then the singular point would be an evolutionary attractor. If the trade-off entered the TIP above the dashed line (the mean curvature of f_1 and f_2) the singular point would be an evolutionary repellor.

For instance, if the trade-off curve entered the TIP below the mutant (f_1) invasion boundary in Fig. 1 then the evolutionary singularity would be an attractor (that is CS and ES). As such the singular point is a 'continuously stable strategy' (CSS) and always the end point of evolution. In contrast, if the trade-off curve entered above the dashed line (mean curvature) of Fig. 1 the singularity would be a repellor (since it is not CS and therefore strains further away from it invade those closer). Thus a visual inspection of the TIP can indicate the type of evolutionary behaviour expected for different trade-off shapes (i.e. by the direction in and strength at which f curves) without the need to specify the trade-off explicitly.

3. Results

3.1. Single species

We begin with a basic maturation model consisting of two stages, a non-reproducing juvenile stage and a reproducing mature stage. This, for two strains x and y, is defined by the continuous time age-structured dynamics

$$\begin{aligned}
\frac{dX_1}{dt} &= a_x X_2 - q_x X_2(X_1+X_2+Y_1+Y_2) - b_x X_1 - m_x X_1,\\
\frac{dY_1}{dt} &= a_y Y_2 - q_y Y_2(X_1+X_2+Y_1+Y_2) - b_y Y_1 - m_y Y_1,\\
\frac{dX_2}{dt} &= m_x X_1 - e_x X_2,\\
\frac{dY_2}{dt} &= m_y Y_1 - e_y Y_2,
\end{aligned} \tag{1}$$

where X_1 and X_2 denote the number of juveniles and matures, respectively, for strain x, and similarly Y_1 and Y_2 for strain y. Also, a represents the per capita reproduction rate of matures (offspring, of course, enter into the juvenile stage), q the rate of intraspecific competition where density-dependence is taken to act on births of juveniles (i.e. of the form $(a-qH)X_2$ with $H=X_1+X_2+Y_1+Y_2$), b and e the death rates of juveniles and matures, respectively, and m the maturation rate which we take to be directly (linearly) related to the number of juveniles.

Calculating the fitness function $s_x(y)$, which defines the long-term exponential growth rate (Metz et al., 1992) of a mutant strain y, of low density, attempting to invade an established resident population of strain x, we get (see Eqs. (A.2)–(A.6))

$$s_x(y) = \frac{1}{b_y+m_y}\left(-b_y + \frac{m_y}{e_y}(a_y - q_y(X_1+X_2) - e_y)\right). \tag{2}$$

From the form for this, with the population equilibrium densities (from Eq. (A.1) which we take to be stable) included explicitly (Eq. (A.7)), and the equivalent form of $s_y(x)$ (found simply by switching the x and y parameters, as y is now the resident and x the invading mutant), we find that the two fitness functions are related by $s_x(y) = -As_y(x)$, where $A>0$. This implies that whenever $s_x(y)$ is positive, $s_y(x)$ is negative, and vice versa. Therefore one strain will always 'win', with no possible co-existence between two strains as the fitness functions can never both be positive simultaneously. In terms of TIPs, this has the consequence that the fitness functions are always zero simultaneously, which in turn, results in the invasion boundaries being identical (i.e. superimposed). From this, we can see that there will be no 'middle' region between the invasion boundaries and hence no possibility of evolutionary branching (see, for example Fig. 2).

As f_1 and f_2 are identical, we will concentrate on the invasion boundary f_1, stemming from $s_x(y)$ being zero. Firstly assuming the trade-off involves the birth rate and is of the form $a=f(\cdot)$, f_1 is, from Eq. (2),

$$a_y = f_1(\cdot) = e_y + \frac{b_y e_y}{m_y} + q_y(X_1+X_2). \tag{3}$$

Taking each of the remaining four parameters in turn to be the second parameter involved in the trade-off, the curvature of the invasion boundaries at the tip of a TIP (and hence their shapes) can be calculated. The first observation we make is that the parameter concerning maturation, m, is the only one that appears non-linearly. The remaining parameters all appear linearly and hence for trade-offs between birth rate a and either one of the death rates, b or e, or the level of intraspecific competition, q, the curvature of f_1 will be zero and hence the invasion boundaries will be straight. In terms of evolutionary outcomes, this means that the singularity is an attractor for accelerating trade-offs and a repellor for decelerating trade-offs. The singular TIPs for these trade-offs will take the form of Fig. 2A. For these trade-offs $f'>0$

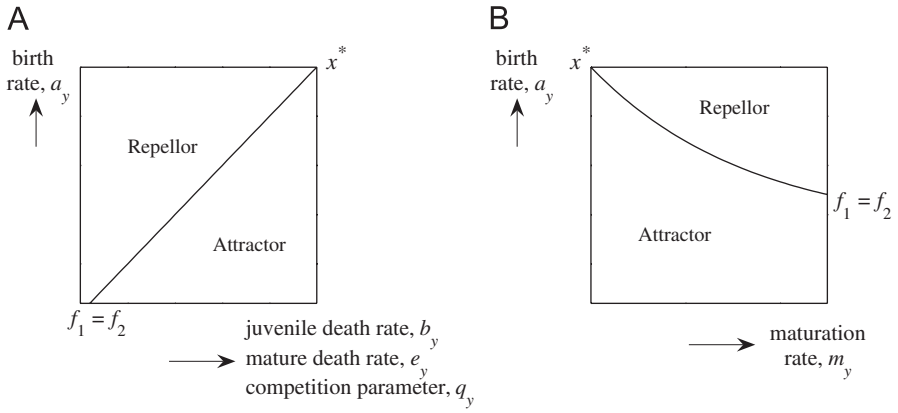

Fig. 2. Singular TIPs for a stage-structured single species maturation model. In (A) the trade-off is between the birth rate, a, and either the death rate of the juveniles or matures or the intraspecific competition parameter, b, e or q, respectively (here $f' > 0$ where $a = f(\cdot)$). In (B) the trade-off is between the birth rate, a, and the maturation rate, m (here $f' < 0$ where $a = f(m)$). Note, here, the direction of the TIPs was chosen to give the most biologically direct representation of the trade-off.

Table 1
Shapes of the invasion boundaries on the singular TIP for all the possible choices of parameters for the trade-off for our single species, stage-structured maturation model

	Mature death rate, e	Maturation rate, m	Competition rate, q	Juvenile death rate, b
Birth rate, a	00 $^=$	DD $^=$	00 $^=$	00 $^=$
Juvenile death rate, b	AA $^=$	00 $^=$	00 $^=$	
Competition rate, q	00 $^=$	DD $^=$		
Maturation rate, m	DD $^=$			

The 'A', 'D' and '0' denote whether the invasion boundaries curve in the manner of an accelerating, decelerating or straight trade-off, respectively, and $^=$ denotes the invasion boundaries being identical (superimposed) in which case branching points are not possible. Note that due to the tangential property of the invasion boundaries about the tip of a TIP, linear invasion boundaries will always be superimposed. The left entry represents the invasion boundary f_1 and the right the invasion boundary f_2. In all cases strongly accelerating costs lead to attractors while strongly decelerating ones result in repellors, while in DD weak decelerating costs lead to attractors and in AA weak accelerating costs are repellors.

(where $a = f(\cdot)$) as a decrease in either the death rate of the juveniles or matures, b or e, or the level of the intrinsic growth rate, q, comes at a cost of a lower birth rate, a. The results for the trade-off between adult birth and survival parallel the findings in classical life-history theory on the evolution of fecundity (Schaffer, 1974; Stearns, 1992). A trade-off with accelerating costs lead to the evolution of intermediate birth and death rates (because the singular point on the TIP is a CSS) whereas one with decelerating costs leads to the evolution of extreme parameter values, such as maximum birth and death rate (because the singular point on the TIP is a repellor).

The remaining choice of trade-off (taken in association with the invasion boundary in Eq. (3)), between the adult birth rate, a, and the maturation rate, m, results in invasion boundaries with positive curvature. In terms of TIPs, f_1 and f_2 curve (but remain superimposed) resulting in a singular TIP of the form as in Fig. 2B. Here $f' < 0$ (where $a = f(m)$) as an increase in the maturation rate, m, comes at a cost of a lower birth rate, a. Here, evolutionary attractors occur not only for accelerating trade-offs but also weakly decelerating trade-offs (and linear trade-offs), whereas evolutionary repellors only occur for strongly decelerating trade-offs. Clearly the relative strength of the costs depends on the relative curvatures of the invasion boundaries. However in general, we use the short hand "weak" where the trade-offs are relatively close to linear.

The results for these four choices of trade-offs considered in Fig. 2 are shown in the top row of Table 1. The letters denote whether the invasion boundaries curve in the same manner as an accelerating trade-off, 'A', a decelerating trade-off, 'D', or are linear/straight, '0'. Since the invasion boundaries are superimposed (the $=$ denotes this), these letters also record the shape of trade-off for which a singularity changes from being an attractor to a repellor. For example, a 'DD' implies that a singularity changes evolutionary outcome depending on the magnitude of a decelerating trade-off, i.e. a repellor for strongly decelerating trade-offs but an attractor for weakly decelerating trade-offs (as in the case of the trade-off between a and m in Fig. 2).

Table 1 also shows the shape of the invasion boundaries for all the remaining possible choices of trade-offs. From this we note that only a small number of trade-off choices in our simple maturation model give curved invasion boundaries on TIPs. These include the birth rate against the maturation rate (a and m), the intraspecific competition rate against the maturation rate (q and m)

and the maturation rate against the death rate of mature individuals (m and e). In these cases evolutionary attractors occur for accelerating trade-offs and weakly decelerating trade-offs, and evolutionary repellors for strongly decelerating trade-offs. In contrast, with a trade-off between the juvenile death rate and the mature death rate (b and e), evolutionary attractors occur for strongly accelerating trade-offs only whereas evolutionary repellors occur for both decelerating trade-offs and weakly accelerating trade-offs. All the remaining possible trade-offs have linear/straight invasion boundaries, and hence evolutionary attractors always occur for accelerating trade-offs and evolutionary repellors for decelerating trade-offs.

3.2. Single class, multi-species interactions

In our remaining models we examine evolution in one species involved in an interaction with another species. To begin with we assume that the dynamics of each species can be described by a single class, the classical examples of which are competition, mutualism and predator–prey. These interactions are all very similar in terms of their dynamics, therefore we aim to set up and use differential equations covering them all and, for predator–prey, examine in turn both prey and predator evolution. Taking two strains of our evolving species, denoted x and y, and a single strain of our non-evolving species, denoted z, gives the Lotka–Volterra form

$$\begin{aligned}
\frac{dX}{dt} &= \delta_1 r_x X - q_x X(X+Y) + \delta_3 c_{xz} XZ,\\
\frac{dY}{dt} &= \delta_1 r_y Y - q_y Y(X+Y) + \delta_3 c_{yz} YZ,\\
\frac{dZ}{dt} &= \delta_2 r_z Z - q_z Z^2 + \delta_3 c_{zx} XZ + \delta_3 c_{zy} YZ,\\
&\text{where } \delta_1,\ \delta_2,\ \delta_3 = \pm 1,
\end{aligned} \tag{4}$$

where X, Y and Z are the population densities of x, y and z, respectively. For the remaining parameters, we take r to represent the intrinsic demographic (growth or mortality) rate of each species/strain, q to be the intra-species interaction (competition) terms and c to be the cross-species interaction terms. The strength of this notation is that by selecting different values of δ_1, δ_2 and δ_3 (see Table 2) Eq. (4) can be made to represent classical competitive, mutualistic and predator–prey systems.

We invoke a relation between the cross-species interaction terms, c_{xz} and c_{zx} (and similarly between c_{yz} and c_{zy}), such that $c_{zx} = g(c_{xz})$ (and similarly $c_{zy} = g(c_{yz})$) (Table 2) in order to model a wide variety of biological scenarios. These interspecific relationships help define the ecological characteristics of the system, in that they, for example, determine how the competition coefficients of two species depend on each other. In the case of predator–prey, we use a standard linear form for g representing a conversion ratio, while in the other cases we can have biologically meaningful positive and negative relationships or indeed no relationship between these terms.

We take the x strain to initially be the resident strain and y to be the mutant invader. In these roles, we can calculate the fitness function $s_x(y)$ as

$$s_x(y) = \delta_1 r_y - q_y X + \delta_3 c_{yz} Z. \tag{5}$$

Here, the fitness can be calculated directly from the dynamics in Eq. (4) as this model consists only of a single class. First taking a trade-off to include the intrinsic growth rate r, the invasion boundary f_1 is, from Eq. (5),

$$r_y = f_1(\cdot) = \frac{1}{\delta_1}(q_y X - \delta_3 c_{yz} Z). \tag{6}$$

We choose the cross-species interaction term, c_{iz}, to be the second parameter involved in the trade-off, so $r_i = f(c_{iz})$, where $i = x$, y and $f' > 0$. Calculating the curvatures of the invasion boundaries at the tip of the singular TIP gives (where Eq. (A.9) was used to calculate the curvature of f_2, also using the equilibrium densities from Eq. (A.8) and the singularity condition $f'|_{x^*} = \partial f_1/\partial c_{yz}|_{x^*}$)

$$\left.\frac{\partial^2 f_1}{\partial c_{yz}^2}\right|_{c_{xz}^*} = 0 \quad \text{and} \quad \left.\frac{\partial^2 f_2}{\partial c_{yz}^2}\right|_{c_{xz}^*} = \left(-\frac{1}{\delta_1}\right)\frac{2q_x g'(c_{xz}^*)X}{[q_x q_z - c_{xz}^* g(c_{xz}^*)]}. \tag{7}$$

The invasion boundary f_1, which stems from $s_x(y)$, is always straight because all the parameters enter the fitness function linearly. Furthermore, the term in square brackets for the curvature of f_2 (in Eq. (7)) is positive due to conditions imposed for the equilibria in Eq. (A.8) to be point stable. Thus, for each interaction, using the appropriate values of δ (and the function $g(c_{xz})$) shown in

Table 2
Sign of the intrinsic growth rate of (evolving) species x (and y), δ_1, and of (fixed) species z, δ_2, sign of the cross-species interaction terms, δ_3, and the relation, with c_{iz}, that the cross-species interaction term c_{zi} takes, for each of our models defined by the dynamics in Eq. (4), namely competition, mutualism and predator–prey (both prey and predator evolution)

Interaction	Sign of the intrinsic growth of species x, δ_1	Sign of the intrinsic growth of species z, δ_2	Sign of the cross-species interaction terms, δ_3	Relation between cross-species interaction terms, c_{zi}, $i = x$, y
Competition	+1	+1	−1	$g(c_{iz})$
Mutualism	+1	+1	+1	$g(c_{iz})$
Prey evolution	+1	−1	−1	$-\beta c_{iz}$
Predator evolution	−1	+1	+1	$-(1/\beta)c_{iz}$

Table 2, we can calculate the shape of the invasion boundaries at the tip of the singular TIP. For competition and mutualism, these are dependent upon the relation between the cross-species interaction terms, primarily on the sign of $g'(c^*_{xz})$ (for predator–prey this is always negative). Results are summarised in Table 3.

The shapes of invasion boundaries specified in Table 3 can be used to produce singular TIPs for the various model systems. Fig. 3 shows the singular TIPs for the competition model for each possible sign of $g'(c^*_{xz})$. If an increase in the competitive ability of one species results in decrease in that of the other species (an aggressive/passive relationship) then there is the possibility of evolutionary branching for trade-offs with weakly decelerating costs (Fig. 3A). If the between species competition parameters are unrelated the invasion boundaries are linear and superimposed (Fig. 3B). If an increase in the between species competition rate of one species results in increase in the other species (aggression is countered with aggression) then a Garden of Eden (ES but not CS) (ES-repellor) outcome exists for weakly accelerating costs (note also that evolutionary branching is no longer possible) (Fig. 3C).

The singular TIPs for mutualism and predator–prey set-ups, with a trade-off between r and c, are similar to those for competition although the specific details are model dependent (and reflect the slope and cost-benefit structure of the trade-off function). For mutualism the singularity is at the top left of the TIP and for predator–prey the TIPs is the same form as Fig. 3A but with the regions being the mirror image in the (straight) f_1 line for predator evolution. For evolutionary branching to occur the between species interaction term must be of the form $g'(c^*_{xz})<0$ (Table 3) reflecting the fact that a benefit through the interaction for one species produces a cost for the other species. If this is the case then branching can occur for trade-offs with weak decelerating costs. For mutualism this requires that an increase in the benefit of the mutualistic interaction for one species produces a reduction in the benefit for the other species. For prey evolution it requires that a reduced predation rate produces fewer predator births and for predator evolution an increased predation rate must increase the loss rate of the prey.

When the interaction term is of the form $g'(c^*_{xz})>0$ reflecting the fact that a benefit through the interaction for

Table 3
Shapes of the invasion boundaries on the singular TIP for our multi-species, single class models, for each possible choice of trade-off and possible sign of $g'(c)$ for competition and mutualism

	Competition	Mutualism	Prey evolution	Predator evolution
Intrinsic growth rate against cross-species interaction (r vs. c)	0A ($g'>0$)	0A ($g'>0$)		
OR	$00^{=}$ ($g'=0$)	$00^{=}$ ($g'=0$)	0D ($g'<0$)	0D ($g'<0$)
Intra-species competition against cross-species interaction (q vs. c)	0D ($g'<0$)	0D ($g'<0$)		
Intrinsic growth rate against intra-species competition (r vs. q)	$00^{=}$	$00^{=}$	$00^{=}$	$00^{=}$

The $g'(c)$ define how a change in interaction coefficient of one species affects that of the other species. In predator/prey interactions the interaction is always antagonistic ($g'<0$), but there may be in addition no relationship ($g'=0$) or a positive relationship ($g'>0$) in both competitive and mutualistic interactions. The 'A', 'D' and '0' denote whether the invasion boundaries curve in the manner of an accelerating, decelerating or straight trade-off, respectively, and $^{=}$ denotes the invasion boundaries being identical (superimposed) in which case branching is not possible. The left entry represents the invasion boundary f_1 and the right the invasion boundary f_2.

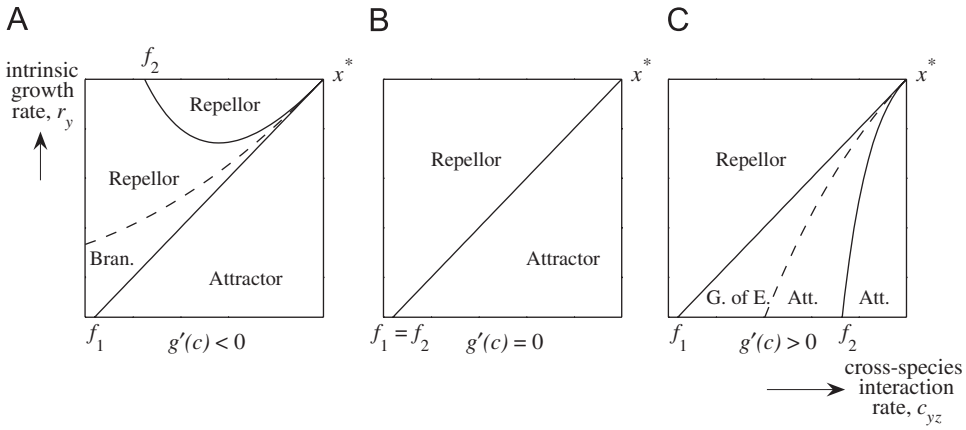

Fig. 3. Singular TIPs for a multi-species, single class competition model, with a trade-off between the intrinsic growth rate, r, and the competition coefficient c (where $r=f(c)$ and $f'>0$). Here the cross-species competition rates are linked by the function $c_{zx}=g(c_{xz})$ and therefore a change in the competitive ability of one species results in a change in the competitive ability in the other. In (A) this between species interaction is such that an increase in the competitive ability of one species leads to a decrease in the ability of its competitor ($g'(c)<0$). In (B) the between species competition terms are independent ($g'(c)=0$). In (C) an increase in the competitive ability of one species leads to an increase in the ability of its competitor ($g'(c)>0$).

one species produces a benefit for the other species then Garden of Eden evolutionary behaviour is possible for trade-offs with weak accelerating costs (in practice these singularities act as evolutionary repellors). When $g'(c^*_{xz}) = 0$, the cross-species interaction terms are unrelated (i.e. there is no interspecific parameter dependence). Here, the two invasion boundaries are identical (superimposed) and hence branching points cannot occur (see also White and Bowers, 2005). Note also that branching requires that the evolving species exhibits intraspecific competition ($q_x > 0$) since otherwise the invasion boundary f_2 is straight and therefore superimposed on f_1 (Eq. (7), see also Bowers et al., 2005).

The remaining two trade-off possibilities are also summarised in Table 3. The trade-off q_x against c_{xz} again involves the cross-species interaction term and produces identical results in terms of the shapes of invasion boundaries and evolutionary outcomes to those for r_x again c_{xz}. The trade-off between r_x and q_x produces two (superimposed) straight invasion boundaries. Here, although the cross-species terms can be related, they are not involved in the trade-off (and are therefore constant) and hence the curvature of the invasion boundaries are equal (and zero) (Bowers et al., 2005; White and Bowers, 2005).

3.3. Multi-species, multi-class

The final section looks at host evolution in a host–parasite model consisting of susceptible and infected classes (with no immune class) where the parasite is therefore modelled implicitly via the infected class of the host. Again taking two strains of host, defined as x and y, we can define the dynamics as follows (based on Anderson and May, 1981):

$$\begin{aligned}
\frac{dS_x}{dt} &= r_x(S_x + kI_x) - q(S_x + kI_x)H - \beta_x S_x(I_x + I_y) \\
&\quad + (\gamma + kb)I_x, \\
\frac{dS_y}{dt} &= r_y(S_y + kI_y) - q(S_y + kI_y)H - \beta_y S_y(I_x + I_y) \\
&\quad + (\gamma + kb)I_y, \\
\frac{dI_x}{dt} &= \beta_x S_x(I_x + I_y) - (\alpha + \gamma + b)I_x, \\
\frac{dI_y}{dt} &= \beta_y S_y(I_x + I_y) - (\alpha + \gamma + b)I_y,
\end{aligned} \tag{8}$$

where $H = S_x + S_y + I_x + I_y$. The parameter r represents the intrinsic growth rate of the host (i.e. births–deaths) and k represents the reduction, due to infection, in the birth rate from infected hosts. For the purposes of this study, we restrict this parameter to either 0, for total loss of reproduction from infecteds (births only from susceptibles), or 1, for no decrease in reproduction due to infection. The parameter q represents competition between hosts, β the infection rate, γ the recovery rate, α the parasite-induced death rate and b the natural death rate where the term $+bkI$ in the susceptible class compensates for the deaths included in rkI.

Due to the added complexity of this model, being both multi-species and multi-class, we present the analysis only for a trade-off between the intrinsic growth rate of the host, r, and the infection rate, β.

As with the two previous examples, for the purposes of calculating the fitness function we take the strains x and y to assume the roles of the established resident and mutant invader, respectively. In these roles, the fitness function, $s_x(y)$, takes the form (see Eqs. (A.11)–(A.14) for working)

$$\begin{aligned}
s_x(y) = \frac{1}{b + \beta_y I_x}\Bigg[& r_y - q(S_x + I_x) \\
& + \frac{\beta_y I_x}{\alpha + \gamma + b}(r_y k - qk(S_x + I_x) - \alpha - (1-k)b)\Bigg].
\end{aligned} \tag{9}$$

We focus on a trade-off of the form $r = f(\beta)$. Finding the invasion boundary f_1, from $s_x(y)$ above, gives

$$r_y = f_1(\beta_y) = q(S_x + I_x) + \frac{\beta_y I_x(\alpha + (1-k)b)}{\alpha + \gamma + b + k\beta_y I_x}. \tag{10}$$

We now go back to the condition we imposed on k, such that we restrict it to the value of 0 or 1 (depending on whether infecteds can reproduce or not), and take these two cases in turn.

Starting with $k = 0$, which relates to the case when there is total loss of reproduction when the host is infected, the curvatures of the invasion boundaries at the tip of the singular TIP are

$$\left.\frac{\partial^2 f_1}{\partial \beta_y^2}\right|_{x*} = 0, \quad \left.\frac{\partial^2 f_2}{\partial \beta_y^2}\right|_{x*} = \frac{2qS_x(\alpha + b)}{\beta^2(\alpha + b + qS_x)}. \tag{11}$$

The main conclusion is that the invasion boundary f_1 is straight, whereas f_2 has positive curvature implying that it curves upwards near the tip of the singular TIP. It follows that the singular TIP will take an identical form to that for competition, in Fig. 3A; hence branching points occur for weakly decelerating trade-offs.

For the second case, we assume there is no reduction in the reproduction rate of the hosts due to infection, hence $k = 1$, and again take a trade-off between the intrinsic growth rate r and the infection rate β. Calculating the curvatures of the invasion boundaries at the tip of the singular TIP gives

$$\begin{aligned}
\left.\frac{\partial^2 f_1}{\partial \beta_y^2}\right|_{x*} &= -\frac{2\alpha S_x I_x^2}{\beta^2(S_x + I_x)^3}, \\
\left.\frac{\partial^2 f_2}{\partial \beta_y^2}\right|_{x*} &= \frac{2\alpha S_x}{\beta^2(S_x + I_x)^3}[-I_x^2 + \theta],
\end{aligned} \tag{12}$$

where θ is as in Eq. (A.15). The invasion boundary f_1 is no longer straight and now curves downwards (Fig. 4). The implication of this is that the evolutionary singularity can be a branching point with either a weakly decelerating

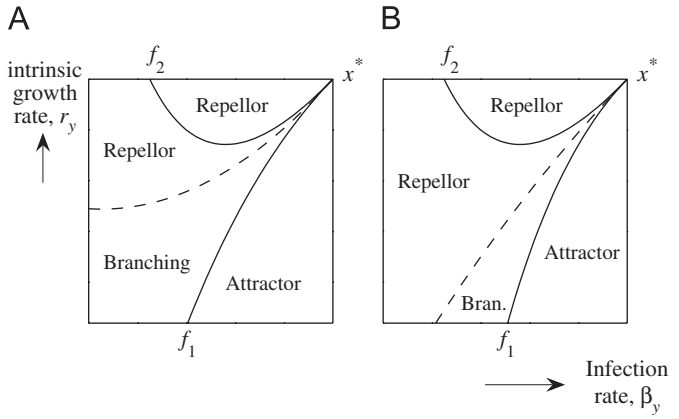

Fig. 4. Singular TIPs for a multi-class, multi-species host–parasite model (with a non-castrating parasite). Here the trade-off is between the intrinsic growth rate r and the infection rate β. In (A) the invasion boundaries have curvature (at the tip) such that the mean curvature (dashed line) is positive, and in (B) they have curvature such that the mean curvature is negative.

trade-off, or a weakly accelerating trade-off (Fig. 4A) or alternatively with a moderately accelerating trade-off (Fig. 4B). This depends upon the relative curvatures of f_1 and f_2. It is important to note that as with all the examples we have seen, evolutionary attractors always occur for strongly accelerating trade-offs and evolutionary repellors for strongly decelerating trade-offs.

The results above emphasise the different configurations of TIPs and therefore evolutionary outcome that can occur. It is interesting to note from Eq. (12) however that, the sign of the curvature of f_2 is also not fixed. Indeed, the curvature can be either greater than or less than that of f_1. Hence these results for when the infecteds can and cannot reproduce emphasise the complex evolutionary outcomes that can be visualised swiftly with the geometric approach.

4. Discussion

The feedback between ecological and evolutionary processes is crucial to understand how ecological interactions generate natural selection and how evolutionary change further modifies the ecological interactions (MacArthur, 1972; Roughgarden, 1979; Bulmer, 1994). By applying a geometric approach we have developed a theory for how different trade-off shapes affect evolutionary outcomes in a number of classical ecological scenarios. The work clearly demonstrates the importance that the shape of the trade-off curve plays. Whether costs are accelerating or decelerating and, furthermore, whether the curvature of these trade-offs is relatively weak or strong (in relation to the invasion boundaries) are key determinants of the evolutionary outcome in all of our examples. The outcomes are also fundamentally dependent on the particular ecological scenario that is being considered. The ecological characteristics of our specific models may change the curvature of both invasion boundaries and therefore radically change the evolutionary outcome but the approach we have taken allows a clear separation of the effects due to the ecological feedbacks and those that result from the shape of the trade-off.

We can define four fundamental forms of TIPs. First, the two invasion boundaries can be linear and therefore superimposed, a type I TIP (see Figs. 2A and 3B). This implies that trade-offs with accelerating costs always produce a CSS, or attractor, while decelerating costs produce a repellor. In type II TIPs, both boundaries curve at the same rate and remain superimposed (see Fig. 2B). Since the curvature of the invasion boundaries can be either positive or negative, the direction and strength of the curvature is important. We find that weakly decelerating costs in addition to accelerating costs can lead to a CSS or in contrast weakly accelerating costs in addition to all decelerating costs can lead to a repellor. It should be noted that whenever the two invasion boundaries are superimposed in our models an optimisation principle exists (Mylius and Diekmann, 1995). This implies that a CSS will produce an intermediate trait value whereas a repellor will always lead to maximisation or minimisation of the trait value. In type III TIPs, one invasion boundary curves while the other remains linear leading inevitably to separation (see Fig. 3A and C). We commonly find that the f_2 boundary curves such that weakly decelerating costs lead to polymorphisms through evolutionary branching, while strong decelerating costs lead to repellors and accelerating costs lead to CSS attractors (although note the alternative configuration of Fig. 3C). Finally in type IV TIP, both boundaries curve but separate (see Fig. 4A and B). Here, we additionally find that weakly accelerating as well as weakly decelerating costs may lead to branching.

Our work emphasises the importance of the strength as well as the nature of the trade-off cost structure. Strong non-linearity always produce CSS or repellor dynamics (for accelerating or decelerating cost structures, respectively) whereas weak non-linearity (and linear trade-offs) can produce the full range of evolutionary behaviour depending on the configuration and type of TIP. It is important to recognise that it is the ecological feedbacks in the system that define the type of TIP that occurs and therefore whether, for example, optimalities or disruptive selection can occur in a particular scenario.

A key aim of our work is to use our models to gain insight into which ecological characteristics lead to each of our fundamental TIPs. To do this we have observed three criteria:

1. Criterion A: The evolving parameters must appear in different classes or one must be repeated, appearing in more than one class/species.
2. Criterion B: The evolving parameters must be characteristics of different classes or one must be a characteristic of more than one class.
3. Criterion C: There must exist two density-dependent per capita rates, each of which must be dependent on different densities.

Satisfying these three criteria in different combinations lead to one of four distinct fundamental TIPs (Table 4).

These criteria hold for the models in this study and allow the range of possible evolutionary behaviour to be predicted by inspection of the model structure and a knowledge of the evolving parameters. The first, criterion A, is that the two evolving parameters must either appear in different classes or one must be repeated, appearing in more than one class/species. Hence, because the two evolving parameters are linked, a change in these parameters will directly affect the dynamics of more than one class/species. Without this, we always get two linear boundaries and therefore a 'simple' optimality (type I). It should be noted that this optimisation can occur in a range of multi-species or multi-class ecological interactions for particular trade-offs. If, in addition to satisfying criterion A, criterion B is satisfied such that the parameters are also characteristics of different classes then the invasion boundaries can curve with equal curvature (type II). For instance in the single species multi-class model (Eq. (1)) the juvenile and mature death rates (b and e, respectively) appear in different classes and are also characteristics of their different respective classes leading to a type II TIP. Contrast this with a trade-off between mature birth and death rates (a and e) which are characteristics of only the mature individuals or birth rate and juvenile death rate (a and b) which appear in the juvenile class only and therefore lead to type I TIPs.

To move from type I or type II TIPs, where the invasion boundaries are superimposed, to type III or type IV TIPs, where they separate, requires criterion C. Whereas criteria A and B focussed on the choice of evolving parameters, criterion C depends only upon the form of the model structure. This criterion is that the dynamics of the evolving species must contain at least two density-dependent per capita rates each of which should be dependent on different densities. Density-dependent rates occur in non-linear model terms. For instance, if we consider prey evolution in a predator–prey system (Eq. (4)) the intraspecific competition term is $-qX^2$ and therefore the rate of intraspecific competition is qX; in the same model the predation term is $-cXZ$ and therefore the rate of predation is cZ. Both the rates are therefore density dependent and are associated with different densities (X and Z, respectively). If criterion C is satisfied the invasion boundaries can separate which allows for the possibility of evolutionary branching. This criterion is analogous to the dimensionality of the fitness environment (Rueffler et al., 2006) however this version has the added benefit that it can be determined directly from inspection of the model without the need for calculating the fitness and hence is easier and quicker to use. Whether we observe type III or type IV TIPs depends on which of the other criteria are satisfied (Table 4) and is best highlighted using the host–parasite model (Eq. (8)). If we consider host evolution, in the presence of a castrating parasite ($k = 0$), then there are two density-dependent rates associated with different densities (the infection rate associated with the density of infecteds, βI, and the intraspecific competition rate associated with total host density, $q(S+I)$) satisfying criterion C. If we consider a trade-off between r and β then criterion A is satisfied (as β appears in both classes) but criterion B is not (as both r and β are characteristics of the susceptible class S). We therefore observe type III TIPs (equivalent to that in Fig. 3A). However when the infected hosts can also reproduce, $k = 1$, criterion B is now satisfied (as r is now also a characteristic of the infecteds I) and so type IV TIPs are observed (Fig. 4). Our three criteria also explain why all the single class, multi-species systems, as described by Eq. (4), can only produce type I or type III TIPs. Criterion C may be satisfied due to the existence of a density-dependent self-regulation rate and the between species interaction rate, however criterion B can never be satisfied because in single class models all evolving parameters are characteristics of a single class. Thus, we can only observe type I or type III TIPs; which of these occur depends on whether the evolving parameters contain the between species interaction parameter (which would allow criterion A to be satisfied).

Although the above insights have only been demonstrated for our models we hypothesise that they will hold in all ecological scenarios that satisfy our constraints. To re-iterate, we restricted these to Lotka–Volterra, continuous time models, i.e. where the evolving parameters appear linearly in the dynamics and the densities are of order 1 or 2. It would be interesting to examine how our conclusions apply to more complex scenarios where, for example, there is a non-linear Holling type II predator

Table 4
Summary of the criteria required to create each of the four types of TIPs

	Criterion A: Trade-off parameters appearing in different classes/species	Criterion B: Trade-off parameters being characteristics of different classes	Criterion C: At least two density-dependent rates which are dependent on different densities
Type IV TIP	✓	✓	✓
Type III TIP	✓	X	✓
Type II TIP	✓	✓	X
Type I TIP	All remaining combinations		

Here type I is two straight invasion boundaries, type II is two curved, superimposed boundaries, type III is one straight and one curved boundary (and therefore separation) and type IV is two curved and separated boundaries.

functional response. However, by initially limiting our work to classical models, we have provided a baseline theory that will at least inform this family of ecological scenarios. Our criteria may therefore allow the rapid evolutionary classification of different trade-offs in a variety of ecological scenarios.

The importance of trade-off shapes in life-history evolution has long been recognised (Levins, 1962). Many of the results from classic life-history theory use optimisation techniques and tend to predict attractors for accelerating trade-offs and repellors for decelerating ones (Stearns, 1992; Roff, 2002). We have shown that this is the case (type I TIP) in our single species system for a number of important trade-offs between life-history components including birth rate verses mature or juvenile death rate. However, there are a number of trade-offs in this model where this result is not found. Strongly accelerating and strongly decelerating trade-offs always lead to the 'classical' results, but when the curvatures are relatively weak they no longer hold (and type II TIPs are possible). We note here that curved invasion boundaries have been reported in life-history examples under adaptation to temporally varying environments (Levins, 1962) and for trade-offs that link multiplicative fitness components (Schaffer, 1974). Our study has shown similar results for a trade-off between two life-history components and highlights the importance of trade-off shapes and the strength of the curvature for a straightforward model framework and trade-off.

For evolutionary branching to occur, not only do criteria A and C need to be satisfied, allowing the invasion boundaries to separate (criterion B is not necessarily needed), but the interaction term between species needs to be antagonistic. Such relationships are obvious in host–parasite and predator–prey systems, where for example the evolution of predator ability clearly affects the prey's ability to avoid predation. For branching to occur in our competitive and mutualistic systems the interaction also has to be antagonistic in the sense that an improvement in one species leads to a reduction in the competitive or mutualistic ability of the other. Clearly not all competitive or mutualistic interactions will be of this type, but one example where we might expect branching is when competition occurs for the same limiting resource. In this case, the uptake of the resource in one competitor will improve its competitive ability and reduce that of the other species (Tompkins et al., 2003). If the competition (or mutualism) coefficients of the two species are independent, or alternatively one competitor can evolve to improve its competitive ability without affecting that of its competitor, there is no possibility of branching. We would therefore predict that there may be more polymorphism and variation in competitive ability when the competition is for a limiting resource.

In the majority of our examples where branching can occur, only one of the invasion boundaries curves with the other one being linear (predator–prey, competition and mutualistic interactions as well as resistance through avoidance when infected individuals do not reproduce, including those parasites that affect immature stages and stop maturation). In these type III TIPs, strongly decelerating costs produce repellors while any degree of acceleration in the costs leads to a CSS. This behaviour has been found in other studies where there is an antagonistic relationship between species. This includes the evolution of size-specific predation on prey life-history (Day et al., 2002) and frequency-dependent selection of consumer types when modelled as evolving specialisation or generalisation on two prey types (Rueffler et al., 2006) (here the underlying ecological scenario is analogous to a predator–prey system). Our study, however, has shown a broader range of behaviour for systems with antagonistic interactions. There are a wide range of castrating parasites in nature including ones that affect immature stages and stop maturation, and for certain trade-offs, for example one between the growth rate of a host and the infection rate, these will produce type III TIPs characteristic of the above antagonistic interactions. However a key ecological characteristic of parasites along with the potential for recovery is that infected individuals do reproduce even if this is at a reduced rate (Boots, 2004; Boots and Norman, 2000). Once reproduction from infecteds occurs, both invasion boundaries may curve, which means that weakly curved cost structures whether decelerating or accelerating may lead to evolutionary branching in resistance (type IV TIP). Cost structures will often depend on specific physiological mechanisms (Boots and Haraguchi, 1999), although intuitively, accelerating costs may be relatively common since gains may tend to saturate quicker than costs. One of the key predictions of our work is that these accelerating costs will lead to a CSS in most antagonistic interactions, but may lead to branching in resistance to parasites where there is either recovery or reproduction by infected individuals. Another example where accelerating costs can induce evolutionary branching is for a multiplicative trade-off in survival in different habitats in which the carrying capacity of each habitat is also dependent on the phenotype (de Mazancourt and Dieckmann, 2004).

Our key result is that shapes of trade-offs matter and that different shapes may have different implications in different scenarios (Levins, 1962, 1968; de Mazancourt and Dieckmann, 2004; Rueffler et al., 2004; Bowers et al., 2005). A broad perspective has been facilitated by the relatively easy way in which the implications of trade-off shapes can be understood using our graphical approach, TIPs. Furthermore, we have defined four fundamental TIPs and are able to identify the ecological characteristics that lead to each of them solely from the dynamics and choice of trade-off. In addition our work particularly emphasises the importance of the strength of the costs, not only in causing disruptive selection leading to branching but also when an optimality principle holds where the invasion boundaries curve. It is clear that trade-off shapes are important and as a consequence, when building

evolutionary models, assumptions about the relationships between traits need to be carefully considered. The outcome will tend to depend heavily on these assumptions. We would therefore argue that this approach may prove useful whenever the implications of trade-off shapes are considered in evolutionary models. Clearly measuring the shape of trade-offs in nature is a major challenge, but we have shown that evolutionary outcomes are crucially dependent on them. There is therefore the pressing need for empirical studies that examine these relationships. Given the controversy surrounding the likelihood of branching in nature (Butlin and Tregenza, 1997) only by measuring these cost structures can we understand how relevant these processes have been in shaping natural communities. It is interesting to note that although many of our scenarios can lead to branching, it is often only found for particular (weak) curvatures. The question of how common branching is likely to be in nature is therefore likely to depend in part on how often key trade-off relationships have these shapes.

Appendix A

A.1. Trade-off and invasion plots

A detailed description of the use of TIPs to determine evolutionary behaviour has been given elsewhere (Bowers et al., 2005). Here we will give a brief outline of TIPs and present some of the results/conditions for determining the evolutionary behaviour of a system. This section provides the mathematical underpinning for the work carried out in this paper.

TIPs are a geometrical approach that makes the role that different trade-off shapes play easy to visualise. Although underpinned mathematically, TIPs are essentially geometrically based, making them a very "user-friendly" method for studying evolution. A TIP is a plot between two (competing) strains of a species, labeled x and y say. One of these, x, is taken to be fixed while the second, y, is allowed to vary. The axes of a TIP are the two evolving parameters of the y strain, y_1 and y_2 (only two parameters are taken to vary). The co-ordinates x_1 and x_2 of the fixed strain x define the corner or tip of a TIP. To emphasise this notation in a biological context consider the evolution of a prey species. Here x_1 and y_1 may represent the prey's ability to avoid predation for two different prey strains while x_2 and y_2 may represent the prey birth rate. An example of a TIP can be seen in Fig. 1.

Two of the three curves on a TIP are the invasion boundaries, denoted as f_1 and f_2. These curves divide a TIP into regions where the varying strain y can and cannot invade the fixed strain x (either side of f_1) and where the fixed strain x can and cannot invade the varying strain y (either side of f_2). If we denote the fitness of a rare mutant y with resident x as $s_x(y)$ (Geritz et al., 1998) then on the curve f_1 we have that $s_x(y)$ is zero and therefore f_1 partitions the TIP into regions where the fitness of strain y is positive and negative. The roles of x and y are reversed when considering the curve f_2 along which $s_y(x)$ is zero. Both of these invasion boundaries pass through the tip of a TIP (a 'neutral' point at which both strains are the same) at which they are tangential. The third curve on a TIP is the trade-off curve, denoted as f; this links the two evolving parameters of each strain. As all feasible pairs of parameters (and hence strains) lie on this curve, f too must pass through the tip of a TIP, but not usually tangentially to the invasion boundaries. Therefore the side of the invasion boundaries in which the trade-off enters a TIP determines whether each strain can invade the other (when initially rare). Generically, the trade-off curve crosses the invasion boundaries at x and so the regular behaviour is invadability of x by y for $y<x$ (say) and non-invadability for $y>x$—with the opposite results for the invadability of y by x (see Bowers et al., 2005).

For certain TIPs corresponding to particular values x^* of x, the trade-off curve can become tangential to the invasion boundaries at the tip of a TIP (i.e. where $y=x=x^*$); then we will have singular behaviour—no change in invadability as we move through x^*. These values of x are evolutionary singularities, with the corresponding TIPs being singular TIPs (Fig. 1). It is from these singular TIPs that the evolutionary behaviour of a system is determined. (If a singular point does not exist, then invadability will prefer either always higher or always lower values of x. If more than one singular point exists then a separate TIP must be considered at each singular point.) Comparing TIPs with $x<x^*$ and $x>x^*$, generically the trade-off curve crosses the invasion boundaries from above in one case and below in the other—the invadability properties change at x^*. Due to the coincidence and mutual tangential property of the three curves at the tip of a singular TIP, the region in which the trade-off curve enters (and hence the evolutionary behaviour) is determined solely by the curvatures of the three curves; or more specifically, the curvature of the trade-off in relation to those of the invasion boundaries at the evolutionary singularity (as in standard theory mutations are assumed to be small). The two significant relations are between the trade-off and f_1 for evolutionary stability (ES) (the criteria for the classical evolutionarily stable strategy (ESS)) and between the trade-off and the mean curvature of both f_1 and f_2 for convergent stability (CS). These can be written as

$$\mathrm{ES} \Leftrightarrow \lambda_1 f''(x^*) < \lambda_1 \left.\frac{\partial^2 f_1}{\partial y_1^2}\right|_{x^*}$$

$$\mathrm{CS} \Leftrightarrow \lambda_1 f''(x^*) < \frac{\lambda_1}{2}\left(\left.\frac{\partial^2 f_1}{\partial y_1^2}\right|_{x^*} + \left.\frac{\partial^2 f_2}{\partial y_1^2}\right|_{x^*}\right),$$

where

$$\lambda_1 = sign\left(\left.\frac{\partial s_x(y)}{\partial y_2}\right|_{x^*}\right).$$

Here λ_1 concerns how the fitness varies as we move vertically up a TIP (i.e. as we vary the parameter on the vertical axis). This determines whether evolutionary attractors occur towards the lower part of a singular TIP (if $\lambda_1>0$) or the upper part (if $\lambda_1<0$). To make this more concrete we observe that, for $\lambda_1>0$, the singularity is ES when the trade-off curve is locally below the f_1 boundary and CS when it is locally below the mean of the two invasion boundaries (this is the situation in the figures presented in this study, but see Table 5 and Bowers et al. (2005) for the $\lambda_1<0$ alternative). Combinations of these properties allow the evolutionary behaviour of the system to be determined. The possible types of singularity are evolutionary attractors or CSS (ES and CS), evolutionary branching point (CS but not an ES), 'Garden of Eden' point or ES-repellor (ES but not CS) and evolutionary repellor (neither ES nor CS).

We close this appendix with two points of clarification on how we draw the TIPs. First, in constructing TIPs we employ biological parameters directly from models performing no transformations on them. Hence the point x may either be in the top right corner (because $f'>0$) or the top left (because $f'<0$). This is exemplified by Fig. 2; in A as the death rate of juveniles increases so does the birth rate; in B as the maturation rate increases the birth rate falls. Second, we display TIPs only for one side of the strategy x: globally every x, y pair is covered exactly once by this procedure, furthermore the geometry of the TIP just above x is determined when that just below x is known and so the evolutionary behaviour is entirely determined by the latter.

Table 5
Summary of the evolutionary outcomes for each shape of trade-off (in relation to the invasion boundaries)

	$\lambda_1\lambda_2>0$	$\lambda_1\lambda_2<0$
$\lambda_2 f''<\lambda_2 f_1''$	Attractor	Repellor
$\lambda_2 f_1''<\lambda_2 f''<\lambda_2$ (*mean*)	Branching point	Garden of Eden point
$\lambda_2 f''>\lambda_2$ (*mean*)	Repellor	Attractor

Here

$$\lambda_1 = sign\left(\left.\frac{\partial s_x(y)}{\partial y_2}\right|_{x^*}\right)$$

(i.e. whether fitness of mutant y increases as we move vertically up a TIP),

$$\lambda_2 = sign\left(\left.\frac{\partial^2 f_2}{\partial y_1^2}\right|_{x^*} - \left.\frac{\partial^2 f_1}{\partial y_1^2}\right|_{x^*}\right)$$

(i.e. whether the f_2 boundary is above or below the f_1 boundary),

$$mean = \frac{1}{2}\left(\left.\frac{\partial^2 f_2}{\partial y_1^2}\right|_{x^*} - \left.\frac{\partial^2 f_1}{\partial y_1^2}\right|_{x^*}\right)$$

(i.e. the mean curvature of the invasion boundaries) and

$$f_i'' = \left.\frac{\partial^2 f_i}{\partial y_1^2}\right|_{x^*}$$

for $i=1,2$.

A.2. Analysis of the models

Starting with the single species, stage-structured model, before any mutations occur, i.e. with only a single (resident) strain x, the population equilibrium densities are

$$X_1 = \frac{e_x(a_x m_x - b_x e_x - m_x e_x)}{q_x m_x(m_x + e_x)},$$
$$X_2 = \frac{a_x m_x - b_x e_x - m_x e_x}{q_x(m_x + e_x)}. \tag{A.1}$$

Our analysis (for all models) is conducted subject to the condition that all feasibility and stability conditions are satisfied. In order for us to calculate the fitness function $s_x(y)$, where the x strain is the existing resident and y the invading mutant, we take the mutant individuals to be in the juvenile stage for an average time T_1 and in the mature stage for an average time T_2. The first of these times, T_1, is given by

$$T_1 = \frac{1}{b_y + m_y}, \tag{A.2}$$

as the only way of leaving the juvenile stage is through death, which occurs at a rate b_y, or through maturation, occurring at a rate m_y. The average time an invader spends in the mature stage, T_2, is found from the equality $b_y T_1 + e_y T_2 = 1$. This stems from the fact that an invading individual can only leave the system through death either as a juvenile or as a mature; this exhausts all possibilities giving a total probability of 1. Solving this for T_2 gives

$$T_2 = \frac{m_y}{e_y(b_y + m_y)}. \tag{A.3}$$

The rates of growth of the mutant population during these times are given by ρ_i ($i=1,\ldots,n$; here $n=2$). These rates are calculated by

$$\rho_i = \lim_{Y_i\to 0}\left(\frac{1}{Y_i}\sum_{j=1}^{n}\left.\frac{dY_j}{dt}\right|_{Y_k=0}\right), \quad \text{where} \quad k=1,\ldots,n \quad \text{and} \quad k\neq i. \tag{A.4}$$

For our juvenile and mature stages, this gives

$$\rho_1 = -b_y,$$
$$\rho_2 = a_y - q_y(X_1 + X_2) - e_y, \tag{A.5}$$

respectively. Combining these in the form $s_x(y) = \rho_1 T_1 + \rho_2 T_2$ gives

$$s_x(y) = \frac{1}{b_y + m_y}\left(-b_y + \frac{m_y}{e_y}(a_y - q_y(X_1 + X_2) - e_y)\right), \tag{A.6}$$

as seen in Eq. (2). Using the equilibrium densities of the juveniles and matures, in Eq. (A.1), the fitness can be

re-arranged into the form

$$s_x(y) = \frac{q_y m_y}{e_y(b_y + m_y)}\left[\left(\frac{a_y - e_y}{q_y} - \frac{b_y e_y}{q_y m_y}\right) - \left(\frac{a_x - e_x}{q_x} - \frac{b_x e_x}{q_x m_x}\right)\right]. \quad (A.7)$$

Moving onto the multi-species, single class model, again initially taking the x strain to be existing alone with species z at equilibrium densities

$$X = \frac{\delta_1 r_x q_z + \delta_2 \delta_3 r_z c_{xz}}{q_x q_z - c_{xz} g(c_{xz})}, \quad Z = \frac{\delta_2 r_z q_x + \delta_1 \delta_3 r_x g(c_{xz})}{q_x q_z - c_{xz} g(c_{xz})}. \quad (A.8)$$

In order to calculate the curvature of the second invasion boundary, at the tip of the singular TIP, we use the result

$$\left.\frac{\partial^2 f_2}{\partial c_{yz}^2}\right|_{x*} = \left.\frac{\partial^2 f_1}{\partial c_{yz}^2}\right|_{x*} + 2\left.\frac{\partial^2 f_1}{\partial c_{xz}\,\partial c_{yz}}\right|_{x*}, \quad (A.9)$$

found by Bowers et al. (2005).

Finally, moving onto our multi-species, multi-class model, we again assume that initially the x strain exists alone. In this scenario, the equilibrium densities for this SIS model are

$$S_x = \frac{\alpha_x + \gamma + b}{\beta_x},$$
$$k = 0 \Rightarrow I_x = \frac{S_x(r_x - qS_x)}{\alpha + b + qS_x},$$
$$k = 1 \Rightarrow I_x = \frac{r_x - \alpha - 2qS_x + \sqrt{(r_x - \alpha)^2 + 2q\alpha S_x}}{2q}, \quad (A.10)$$

where we have two possible equilibrium densities for the infecteds depending upon whether they can produce (susceptible) offspring at an identical rate to the susceptibles or not at all. As this is a two class model, we again need to calculate the rates of growth of the host population while the invader is in each class, ρ_S (susceptible) and ρ_I (infected), and also the average time a mutant individual spends in each class, T_S (susceptible) and T_I (infected). Starting with the times, as the only way of leaving the susceptible class is through (natural) death or infection, we can write down the average time an invader spends in this class as

$$T_S = \frac{1}{b + \beta_y I_x}. \quad (A.11)$$

The average time an invader spends in the infected class is derived from the equality $bT_S + (\alpha + \gamma + b)T_I = 1$, which is similar to the method for maturation. Solving this for T_I gives

$$T_I = \frac{\beta_y I_x}{(b + \beta_y I_x)(\alpha + \gamma + b)}. \quad (A.12)$$

Now, using (A.4) to find the rates of growth while the invader is in the susceptible and the infected classes gives

$$\rho_S = r_y - q(S_x + I_x),$$
$$\rho_I = r_y k - qk(S_x + I_x) - \alpha - (1 - k)b. \quad (A.13)$$

Combining these in such a way that the fitness function takes the form $s_x(y) = \rho_S T_S + \rho_I T_I$ gives

$$s_x(y) = \frac{1}{b + \beta_y I_x}\left[r_y - q(S_x + I_x) + \frac{\beta_y I_x}{\alpha + \gamma + b} \times (r_y k - qk(S_x + I_x) - \alpha - (1 - k)b)\right]. \quad (A.14)$$

In further manipulation based on this quantity (with a trade-off between r and β and a non-castrating parasite) we find it convenient to use the quantity

$$\theta = S_x(S_x - I_x)\left(1 - \frac{\alpha S_x}{(S_x + I_x)\sqrt{(r - \alpha)^2 + 4q\alpha S_x}}\right), \quad (A.15)$$

in the main text.

References

Abrams, P., 2001. Modelling the adaptive dynamics of traits in inter~ and intraspecific interactions: an assessment of three models. Ecol. Lett. 4, 166–175.

Anderson, R.M., May, R.M., 1981. The population dynamics of microparasites and their invertebrate hosts. Philos. Trans. R. Soc. London 291, 451–524.

Boots, M., 2004. Modelling insect diseases as functional predators. Physiol. Entomol. 29, 237–239.

Boots, M., Bowers, R.G., 2004. The evolution of resistance through costly acquired immunity. Proc. R. Soc. London B 271, 715–723.

Boots, M., Haraguchi, Y., 1999. The evolution of costly resistance in host–parasite systems. Am. Nat. 153, 359–370.

Boots, M., Norman, R., 2000. Sublethal infection and the population dynamics of host–microparasite interactions. J. Anim. Ecol. 69, 517–524.

Bowers, R.G., White, A., Boots, M., Geritz, S.A.H., Kisdi, E., 2003. Evolutionary branching/speciation: contrasting results from systems with explicit or emergent carrying capacities. Evol. Ecol. Res. 5, 883–891.

Bowers, R.G., Hoyle, A., White, A., Boots, M., 2005. The geometric theory of adaptive evolution: trade-off and invasion plots. J. Theor. Biol. 233, 363–377.

Bulmer, M., 1994. Theoretical Evolutionary Ecology. Sinauer Associates, Sunderland, MA.

Butlin, R.K., Tregenza, T., 1997. Evolutionary biology: is speciation no accident? Nature 387, 551–552.

Day, T., Abrams, P.A., Chase, J., 2002. The role of size-specific predation in the evolution and diversification of prey life histories. Evolution 56, 877–887.

De Mazancourt, C., Dieckmann, U., 2004. Trade-off geometries and frequency-dependent selection. Am. Nat. 164, 765–778.

Egas, M., Dieckmann, U., Sabelis, M.W., 2004. Evolution restricts the coexistence of specialists and generalists—the role of trade-off structure. Am. Nat. 163, 518–531.

Geritz, S.A.H., Kisdi, E., Meszena, G., Metz, J.A.J., 1998. Evolutionary singular strategies and the adaptive growth and branching of the evolutionary tree. Evol. Ecol. 12, 35–57.

Kisdi, E., 2001. Evolutionary branching under asymmetric competition. J. Theor. Biol. 197, 149–162.

Levins, R., 1962. Theory of fitness in heterogeneous environment. 1. The fitness set and the adaptive function. Am. Nat. 96, 361–373.

Levins, R., 1968. Evolution in Changing Environments. Princeton University Press, Princeton, NJ.

MacArthur, R.H., 1972. Geographical Ecology. Harper & Row, New York.

Maynard Smith, J., 1982. Evolution and the Theory of Games. Cambridge University Press, Cambridge.

Metz, J.A.J., Nisbet, R.M., Geritz, S.A.H., 1992. How should we define 'fitness' for general ecological scenarios? Trends Ecol. Evol. 7, 198–202.

Metz, J.A.J., Geritz, S.A.H., Meszena, G., Jacobs, F.J.A., Van Heerwaarden, J.S., 1996. Adaptive dynamics: a geometric study of the consequences of nearly faithful reproduction. In: van Strein, S.J., Verduyn Lunel, S.M. (Eds.), Stochastic and Spatial Structures of Dynamical Systems. Proceedings of the Royal Dutch Academy of Science (Verhandelingen KNAW). North-Holland, Amsterdam, pp. 183–231.

Mylius, S.D., Diekmann, O., 1995. On evolutionary stable life histories, optimisation and the need to be specific about density-dependence. Oikos 74, 218–224.

Roff, D.A., 2002. Life History Evolution. Sinauer Associates, Sunderland, MA.

Roughgarden, J., 1979. Competition and theory in community ecology. Am. Nat. 5, 583–601.

Rueffler, C., Van Dooren, T.J.M., Metz, J.A.J., 2004. Adaptive walks on changing landscapes: Levin's approach. Theor. Popul. Biol. 65, 165–178.

Rueffler, C., Van Dooren, T.J.M., Metz, J.A.J., 2006. The evolution of resource specialization through frequency-dependent and frequency-independent mechanisms. Am. Nat. 167, 81–93.

Schaffer, W.M., 1974. Optimal reproductive effort in fluctuating environments. Am. Nat. 108, 783–790.

Stearns, S.C., 1992. The Evolution of Life Histories. Oxford University Press, Oxford.

Tompkins, D., White, A., Boots, M., 2003. Ecological replacement of native red squirrels by invasive greys driven by disease. Ecol. Lett. 6, 189–196.

White, A., Bowers, R.G., 2005. Adaptive dynamics of Lotka–Volterra systems with trade-offs: the role of intraspecific parameter dependence in branching. Math. Bios. 197, 101–117.